

MACROMOLECULAR CROWDING ENHANCES FIBRILLIN-1 DEPOSITION IN THE EXTRACELLULAR MATRIX

B. Satz-Jacobowitz¹, N. Taye¹, S. Z. Karoulias^{1,2} and D. Hubmacher^{1,*}

¹Orthopaedic Research Laboratories, Leni & Peter W. May Department of Orthopaedics, Icahn School of Medicine at Mount Sinai, New York, NY, 10029, USA

²Present address: Regeneron, Tarrytown, NY, 10591, USA

Abstract

Biochemical and biophysical factors need consideration when modelling *in vivo* cellular behaviour using *in vitro* cell culture systems. One underappreciated factor is the high concentration of macromolecules present *in vivo*, which is typically not simulated under standard cell culture conditions. This disparity is especially relevant when studying biochemical processes that govern extracellular matrix (ECM) deposition, which may be altered due to dilution of secreted macromolecules by the relatively large volumes of culture medium required for cell maintenance *in vitro*. Macromolecular crowding (MMC) utilises the addition of inert macromolecules to cell culture medium to mimic such high concentration environments found *in vivo*. The present study induced MMC using the sucrose polymer Ficoll and examined whether fibrillin-1 deposition by human lung fibroblasts could be augmented. Fibrillin-1 forms extracellular microfibrils, which are versatile scaffolds required for elastic fibre formation, deposition of other ECM proteins and growth factor regulation. Pathogenic variants in the fibrillin-1 gene (*FBN1*) cause Marfan syndrome, where ECM deposition of fibrillin-1 can be compromised. Using immunocytochemistry, significantly enhanced fibrillin-1 deposition was observed when lung fibroblasts were cultured under MMC conditions. MMC also augmented fibrillin-1 deposition in Marfan syndrome patient-derived skin fibroblasts in a cell line- and likely *FBN1* variant-specific manner. The ability of MMC to increase fibrillin-1 deposition suggested potential applications for tissue-engineering approaches, *e.g.* to generate tendon or vascular tissues, where fibrillin-1 microfibrils and elastic fibres are key determinants of their biomechanical properties. Moreover, it suggested the potency of MMC to better mimic *in vivo* ECM environments in cell culture studies.

Keywords: Macromolecular crowding, tissue engineering, elastic fibres, Marfan syndrome, microfibrils.

***Address for correspondence:** Dirk Hubmacher, Department of Orthopaedics, Icahn School of Medicine at Mount Sinai, 1468 Madison Avenue, New York, NY, 10029, USA.

Telephone number: +1 2122411625 Email: dirk.hubmacher@mssm.edu

Copyright policy: This article is distributed in accordance with Creative Commons Attribution Licence (<http://creativecommons.org/licenses/by/4.0/>).

List of Abbreviations

ANOVA	analysis of variance	PBS	phosphate-buffered saline
BMP	bone morphogenetic protein	PVDF	poly-vinylidene difluoride
DAPI	4',6-diamidino-2-phenylindole	RT	room temperature
DMEM	Dulbecco's modified Eagle medium	SDS	sodium dodecyl sulphate
ECM	extracellular matrix	TBS	Tris-buffered saline
<i>FBN1</i>	fibrillin-1 (gene)	TBS-T	TBS + 0.1 % Tween 20
FBS	foetal bovine serum	TGFβ	transforming growth factor β
FITC	fluorescein isothiocyanate		
GAPDH	glyceraldehyde 3-phosphate dehydrogenase		
LTBP	latent transforming growth factor β binding protein		
MMC	macromolecular crowding		
PAGE	polyacrylamide gel electrophoresis		

Introduction

The biophysical and biomechanical properties required for tissue function of tendons, blood vessels, lungs, skin, *etc.* are largely defined by the dense ECM, which is synthesised and remodelled by tissue resident cells (Karamanos *et al.*, 2021; Taye *et al.*, 2020;

Theocharis *et al.*, 2019). Consequently, most cells are surrounded *in vivo* by tissue-specific combinations of various ECM proteins, including fibrillins, elastin, collagens, proteoglycans and glycosaminoglycans as well as latent and active signalling molecules. As a result, the microenvironment surrounding the cells contains a high concentration of macromolecules, *i.e.* is crowded (Mecham and Heuser, 1990). Because cell culture medium lacks the diversity and density of molecules surrounding cells *in vivo*, innovation in cell culture requires an appreciation of how these concentrated extracellular environments impact cell behaviour. While a perfect replication of these *in vivo* cell environments may prove unattainable in cell culture settings, inert macromolecules can be added to artificially enhance the concentration of secreted macromolecules in cell culture and, thus, guide biological processes, such as ECM deposition, which are frequently concentration dependent. This approach is called MMC and is designed to more faithfully model cellular *in vivo* microenvironments *in vitro* (Ellis, 2001; Zeugolis, 2021).

MMC centres on the principle of volume exclusion by inert macromolecules, where a high concentration of macromolecules results in a reduction in available space to be occupied by soluble components secreted by cells in culture (Tsiapalis and Zeugolis, 2021). This reduction in available volume promotes biochemical interactivity through spatial confinement. The concept was initially described in the early 1960s by A.G. Ogston, who studied the capacities of hyaluronic acid to reduce the solubility of inulin and other molecules by steric or volume exclusion (Ogston and Phelps, 1960; 1961). Laurent (1963) showed that the addition of the uncharged polysaccharides dextran and Ficoll to solutions of albumin, γ -globulin, fibrinogen or α -crystallin decreases the solubility of these proteins. These experiments were designed to model the high macromolecular density in the ECM and investigate how it might affect deposition of proteins such as ECM components.

The range of processes impacted by MMC-mediated volume exclusion has experimentally been shown to include protein folding, DNA replication, DNA transcription, rate of enzymatic reactions, protein-protein interaction and cell function (Rivas and Minton, 2016; Tsiapalis and Zeugolis, 2021). The higher effective concentrations of molecules alter the rates and equilibrium constants of their reactions and promote association between them. Thus, MMC affects not only protein solubility but also protein interactivity, enhancing reaction rates by several orders of magnitude. In the ECM, expedited collagen deposition is a function of several MMC thermodynamic effects, including optimisation of protein folding, enhanced proteolytic procollagen processing, increased protein aggregation, as well as polymerisation, of monomers and decreased solubility to accelerate deposition of mature collagen fibres (Chen *et al.*, 2013; Gaspar *et al.*, 2019; Graham *et al.*, 2019; Lareu *et al.*, 2007).

Prior literature documented enhanced deposition of collagen types I, III, IV, V and VI and of fibronectin in the presence of MMC reagents (Garnica-Galvez *et al.*, 2021; Kumar *et al.*, 2015). However, very limited data are available on how MMC affects deposition of other structural ECM components, such as fibrillin-1. The motivations to investigate the role of MMC in fibrillin-1 deposition follow its importance as an ECM scaffolding molecule for components of the elastic fibre system and its involvement in Marfan syndrome. Fibrillin-1 is a structural ECM protein that forms microfibrils in a hierarchical assembly process requiring multimerisation, N-to-C-terminal self-interactions and ECM deposition on a fibronectin template in mesenchymal cells (Hubmacher *et al.*, 2008; Lin *et al.*, 2002; Sabatier *et al.*, 2009). Fibrillin-1 microfibrils serve as a scaffold for elastin deposition and elastic-fibre formation. Moreover, microfibrils are required for the ECM deposition of proteins, such as LTBPs, fibulins and BMPs (El-Hallous *et al.*, 2007; Kumra *et al.*, 2019; Sengle *et al.*, 2008; Zilberberg *et al.*, 2012). As such, fibrillin-1 not only endows connective tissue integrity but also directly participates in TGF β and BMP signalling regulation. Pathogenic variants of *FBN1* can cause connective tissue disorders, such as Marfan syndrome, Weill-Marchesani syndrome or geleophysic dysplasia (Dietz *et al.*, 1991; Faivre *et al.*, 2003; Le Goff *et al.*, 2011; Stanley *et al.*, 2020). Since fibrillin-1 microfibrils are mediators of elastic-fibre formation, promoting fibrillin-1 microfibril formation in the ECM could be an important step for the successful engineering of elastic tissues, such as tendon or blood vessels, where elastic fibres, together with collagens and proteoglycans, determine their biomechanical properties.

Using human lung fibroblasts and Marfan syndrome patient-derived skin fibroblasts, it was determined that MMC augmented fibrillin-1 deposition – specifically early in the cell-culture period – in the ECM of lung fibroblasts and some Marfan syndrome fibroblasts. In addition, fluorescently labelled Ficoll could be detected in the cell layer, raising the possibility that it may interfere with some processes in the ECM or in the pericellular matrix.

Materials and Methods

Cell culture

Human lung fibroblasts (WI-38, American Type Culture Collection) were cultured on 100 mm cell culture dishes (Corning Falcon) in DMEM (ThermoFisher Scientific) containing 1 % L-glutamine, 10 % FBS, 100 units/mL penicillin and 100 μ g/mL streptomycin (complete DMEM). Cells were incubated at 37 °C and 5 % CO₂ in a humidified incubator and medium was changed every 3-4 d. Primary human dermal fibroblasts derived from Marfan syndrome patients were purchased from the

Table 1. Molecular characteristics of Marfan syndrome patient-derived skin fibroblasts. ¹ Nomenclature based on the fibrillin-1 RefSeq NM_000138.5. ² Numbering based on RefSeq NP_000129.

Coriell ID	FBN1 exon	FBN1 variant ¹	Fibrillin-1 amino acid change ²	Age at sampling/sex	Reference
GM21932	38	c.4766G>T	p.Cys1589Phe	25 years / male	Tynan <i>et al.</i> (1993)
GM21954	15	c.1909T>C	p.Cys637Arg	13 years / male	Schrijver <i>et al.</i> (1999)
GM21966	7	c.745G>T	p.Glu249*	67 years / male	Schrijver <i>et al.</i> (2002)
GM21989	50	c.6283insC	p.Asp2104*	22 years / male	Schrijver <i>et al.</i> (2002)

Coriell Institute for Medical Research (Camden, NJ, USA) and were cultured as described above (Table 1).

MMC

Ficoll 70 (GE-0310-10) and Ficoll 400 (F8016) were purchased from Sigma-Aldrich and lambda-Carrageenan (C331325g) was purchased from Thermo Fisher Scientific. Ficoll is a high molecular weight, non-ionic, highly branched, sucrose polymer with low osmolarity and low membrane permeability, synthesised by copolymerisation of sucrose and epichlorohydrin. Ficoll is hydrophilic due to a high hydroxyl content and is stable in aqueous solutions at alkaline and neutral pH. Ficoll 70 and Ficoll 400 were dissolved at a concentration of 62.5 mg/mL in DMEM by vigorous vortexing, as previously described (Zeiger *et al.*, 2012). Complete DMEM containing Ficoll was stored at 4 °C and used within 10 d. The Ficoll mix was prepared by dissolving Ficoll 70 and Ficoll 400 in complete DMEM at a ratio of 60:40 (w/w) (37.5 mg/mL and 25 mg/mL, respectively). Lambda-Carrageenan is an anionic mucopolysaccharide derived from red algae that does not gel or form helical structures. It was dissolved in complete DMEM at concentrations ranging from 10 µg/mL to 200 µg/mL (De Pieri *et al.*, 2020). The MMC reagents were added 24 h after cell seeding and replenished, together with fresh complete DMEM, after 3 d for the 7 d culture period. Ficoll 70 (FP70) and Ficoll 400 (FP400) conjugated with FITC were purchased from TdB Labs (Uppsala, Sweden) and prepared and applied as described above.

Immunocytochemistry staining

50,000 cells per well (38,000 cells/cm²) were seeded in 8-well chamber slides (CELLTREAT Scientific Products, Pepperell, MA, USA) and cultured in 0.5 mL complete DMEM. This cell density allows for the synthesis of a robust ECM, including fibrillin-1 fibres, but is somewhat lower than in previous reports using primary Marfan syndrome patient-derived fibroblasts (Balic *et al.*, 2021; Godfrey *et al.*, 1995; Hubmacher *et al.*, 2005; Raghunath *et al.*, 1993; Sabatier *et al.*, 2009). For both the 4 d and 7 d culture periods, MMC reagents dissolved in complete DMEM were added 24 h after seeding. For the 7 d

culture period, the medium was replenished with fresh Ficoll-containing complete DMEM 4 d after seeding. 4 or 7 d after seeding, *i.e.* 3 and 6 d of MMC/Ficoll treatment, the medium was removed, cells were rinsed once in PBS and fixed using ice-cold 70 % methanol/30 % acetone (v/v) for 5 min. Fixed cells were rinsed again in PBS and blocked for 1 h at RT in 10 % normal goat serum in PBS (blocking buffer). Cells were subsequently incubated for 2 h at RT with primary antibodies raised against fibrillin-1 (polyclonal, 1:1,000) and fibronectin (clone FN-15, 1:500, Sigma-Aldrich, F7387) diluted in blocking buffer. The polyclonal antiserum against the C-terminal half of fibrillin-1 has been described previously (Tiedemann *et al.*, 2001). Cells were rinsed 3 × 5 min in PBS before incubation for 2 h at RT with the secondary antibodies goat-anti-mouse Alexa-488 and goat-anti-rabbit rhodamine red X, diluted 1:200 (Jackson ImmunoResearch Laboratories) in blocking buffer. Finally, cells were rinsed 3 × 5 min in PBS and mounted on microscope slides using the ProLong Diamond Antifade Mountant containing DAPI nuclear stain (ThermoFisher Scientific). The slides were imaged using a Zeiss Axio Observer Z1 Fluorescence Motorized Microscope w/ Definite Focus.

Quantification and analysis of immunocytochemistry images

Fluorescence intensities from the individual channels were extracted using the ZEISS ZEN lite software (Zeiss) and fluorescence intensity profiles were generated using Fiji/ImageJ (Schindelin *et al.*, 2012). Arithmetic mean pixel intensities for each fluorescence channel in each of the images were normalised to the corresponding arithmetic mean pixel intensity of the DAPI signal as a surrogate for cell number. Parameters for ECM networks, including number of branches and number of junctions were determined using Fiji/ImageJ as described recently (Zhang *et al.*, 2020). Briefly, images from individual channels were despeckled 3 times to remove background noise and the “Skeletonize (2D/3D)” plugin followed by the “Analyze Skeleton” were applied to determine the number of branches and junctions as markers of ECM network complexity.

SDS-PAGE and Western blotting

300,000 cells per well (31,600 cells/cm²) were seeded in 6-well plates (Corning Falcon) and cultured in the presence or absence of Ficoll 400 in serum-free DMEM. After 4 d (3 d with Ficoll 400), culture medium was collected and cleared from cell debris by centrifugation at 15,000 ×g for 5 min at 4 °C. 56 µL of supernatant were combined with 14 µL of 5× reducing SDS-PAGE loading buffer (0.5 mol/L Tris pH 6.8, 5 % 2-mercaptoethanol, 20 % SDS, 1 % bromophenol blue, 50 % glycerol) and incubated for 5 min at 95 °C. The cell layer was rinsed once with 1 mL PBS, lysed using 100 µL lysis buffer (0.1 % NP40, 0.01 % SDS, 0.05 % Na-deoxycholate in PBS), removed using a cell scraper (CELLTREAT Scientific Products, Pepperell, MA, USA) and transferred into an Eppendorf tube. After 5 min incubation, cell lysates were centrifuged at 15,000 ×g for 15 min at 4 °C. The supernatant was combined with 25 µL 5× SDS-PAGE loading buffer and incubated at 95 °C for 5 min.

The denatured proteins from culture media or cell lysates were separated on a 6 % polyacrylamide gel by SDS-PAGE using a Mini-PROTEAN Tetra Electrophoresis System (Bio-Rad) run at 90 mV for 30 min and 120 mV until completion. Then, the proteins were transferred from the gel onto PVDF membranes (Immobilon-FL, Merck Millipore) by wet transfer at 70 mV for 1.5 h using a 25 mmol/L Tris, 192 mmol/L glycine and 20 % methanol transfer buffer. Following transfer, membranes were blocked for 1 h using 5 % (w/v) non-fat dry milk in TBS (10 mmol/L Tris-HCl, pH 7.2, 150 mmol/L NaCl).

The primary antibodies against fibrillin-1 and fibronectin were used at a 1:500 dilution in 5 % milk in TBS + 0.1 % Tween 20 (TBS-T) overnight at 4 °C. GAPDH, detected using the monoclonal antibody MAB374 (1:500, Sigma-Aldrich), was utilised for normalisation. Following incubation with primary antibodies, membranes were washed 3 × 5 min with TBS-T at RT, followed by incubation with the secondary antibodies IRDye goat-anti-mouse (green) and IRDye goat-anti-rabbit (red) (1:10,000, LI-COR) diluted in 5 % (w/v) non-fat dry milk in TBS-T for 2 h at RT. After incubation, blots were rinsed 3 × 5 min in TBS-T, 1 × 5 min in TBS and 1 × 5 min in water.

Membranes were imaged using a LI-COR Odyssey Classic Imaging System (LI-COR Biosciences). Quantification and densitometric analysis were conducted using Fiji/ImageJ software where the red and green fluorescence of individual bands were quantified through colour histogram analysis and GAPDH bands through mean grey intensity. Fibrillin-1 and fibronectin band intensities were normalised to GAPDH.

Statistical analysis

Statistical analysis was performed using OriginPro 2019 software (OriginLab Corporation, Northampton, MA, USA). Pairwise comparisons were evaluated using two-sample Student's *t*-test. One-way ANOVA

followed by a *post-hoc* Tukey test was used to compare multiple groups. Statistical significance was considered for $p < 0.05$. Experiments were performed at least in biological triplicates and multiple fields of view were analysed.

Results

MMC with Ficoll promoted fibrillin-1 deposition after a 4 d culture period

The effects of the two MMC reagents, Ficoll 70 and Ficoll 400, on fibrillin-1 deposition in the ECM of human lung fibroblasts were investigated. Ficoll 70 and Ficoll 400 are non-ionic, highly branched sucrose polysaccharides of 70 ± 10 kDa and 400 ± 100 kDa molecular weight, respectively, previously used in MMC experiments either individually or in combination in a 60:40 (w/w) ratio, referred to from here on as Ficoll mix (Chen *et al.*, 2011; Gaspar *et al.*, 2019). Fibrillin-1 and fibronectin deposition, the latter being required for fibrillin-1 deposition in fibroblasts, were visualised by immunostaining (Sabatier *et al.*, 2009). When Ficoll 400 was added, fibrillin-1 deposition in the ECM was significantly increased compared to untreated controls after 4 d in culture, *i.e.* 3 d following addition of the MMC reagent (Fig. 1a,b). MMC treatment with either Ficoll 70 or Ficoll mix showed non-significant changes in fibrillin-1 deposition in the ECM (Fig. 1a,b). Fibronectin deposition was also significantly increased upon treatment with Ficoll 400, but not with Ficoll 70 or Ficoll mix (Fig. 1a,b). However, the fold-increase of fibronectin was lower compared to fibrillin-1. Fibrillin-1 and fibronectin networks deposited in the presence or absence of MMC reagents were additionally analysed for parameters characterising ECM network complexity (Zhang *et al.*, 2020). The numbers of branches and junctions in fibrillin-1 networks were significantly increased under all MMC conditions, indicative of a denser ECM network (Fig. 1c,d). However, the strongest increase was observed with Ficoll 400, which caused a significantly larger increase compared to Ficoll 70 or Ficoll mix conditions. The fibronectin ECM network showed significant increases in branch numbers when Ficoll 400 or Ficoll mix, but not Ficoll 70, were added and significant changes in the number of junctions under all conditions (Fig. 1c,d). Similar to the fibrillin-1 network parameters, the increases were most pronounced after treatment with Ficoll 400.

To determine if the amount of fibrillin-1 or fibronectin protein changed, the cell/ECM lysates and conditioned media harvested from Ficoll 400-treated as well as untreated lung fibroblasts were analysed by semi-quantitative Western blotting (Fig. 1e,f). Densitometric analysis demonstrated a significant decrease in the amount of soluble fibrillin-1 protein in conditioned medium of lung fibroblasts when treated with Ficoll 400, compared to untreated controls (Fig.

1f). The amount of fibrillin-1 and fibronectin present in the cell lysate/ECM layer showed higher variability amongst the various conditions but collectively no statistically significant changes in the band intensities were observed.

Fibrillin-1 deposition was not further enhanced with Ficoll after a 7 d culture period

To test if fibrillin-1 deposition could be further enhanced by prolonged culture periods in the presence of MMC reagents, fibrillin-1 and fibronectin

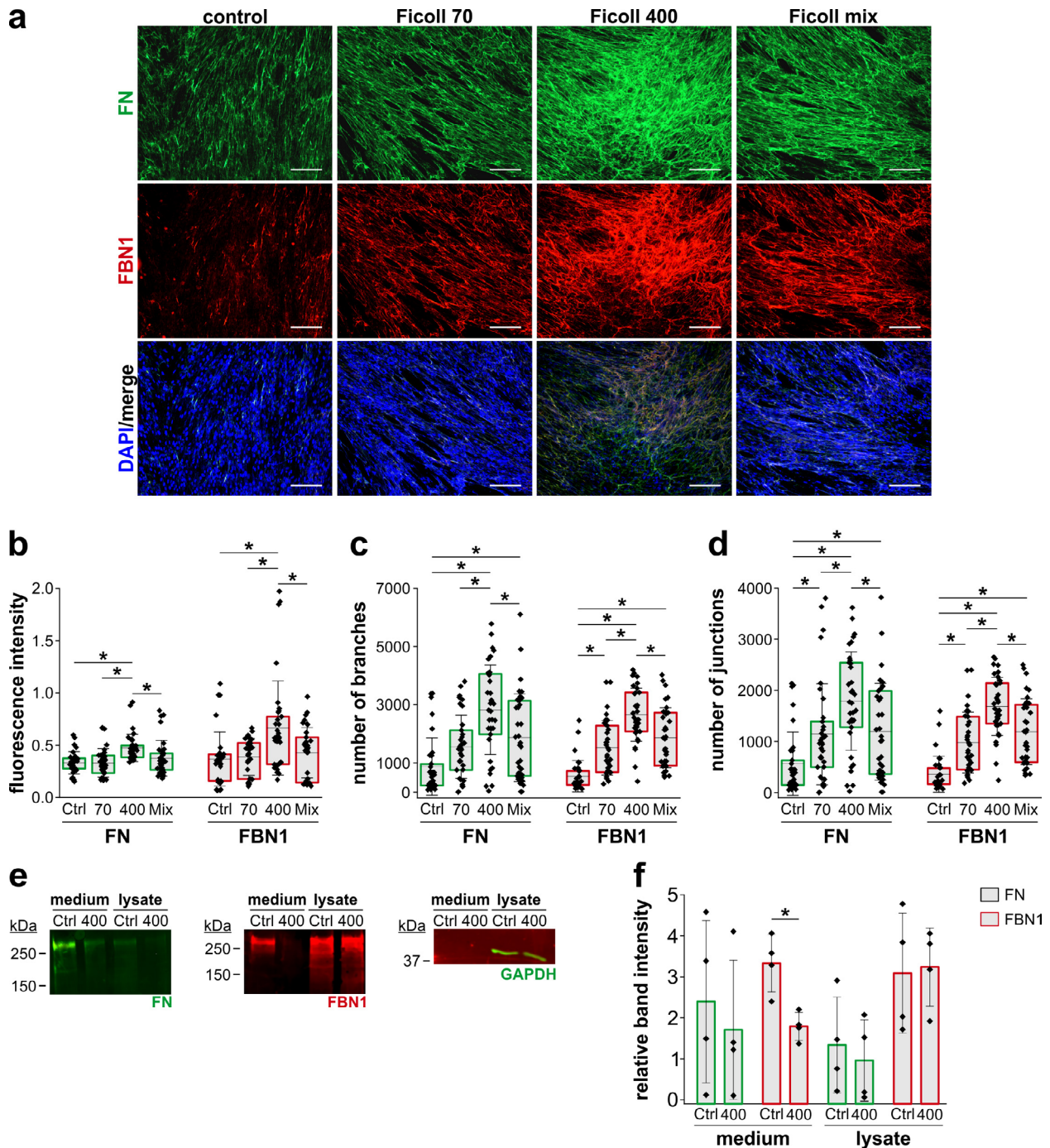


Fig. 1. MMC with Ficoll promoted fibrillin-1 deposition in 4 d cultures. (a) Representative images of indirect immunofluorescence staining for fibronectin (FN) and fibrillin-1 (FBN1) deposited by lung fibroblasts after 3 d in the absence (Ctrl) or presence of Ficoll 70 (70), Ficoll 400 (400) or Ficoll mix (Mix). Nuclei were stained with DAPI. Scale bars = 200 μ m. Quantification of (b) fluorescence intensity normalised to DAPI, (c) number of branches and (d) number of junctions. Boxes represent the 25th-75th percentile range and whiskers the standard deviation. Individual data points represent 4-10 fields of view for each condition from $n = 3-4$ independent experiments. (e) Western blot analysis of FN, FBN1 and GAPDH protein quantity in conditioned medium and cell lysate from untreated or Ficoll 400-treated lung fibroblasts. (f) Quantification of band intensity from FN and FBN1 after Western blotting normalised to GAPDH ($n = 4$). Statistical analysis was performed using a (b-d) one-way ANOVA followed by *post-hoc* Tukey test or a (f) two-sample Student's *t*-test. * $p < 0.05$ was considered statistically significant.

ECM deposition were analysed after 7 d in culture, *i.e.* 6 d of Ficoll treatment with one medium change to replenish nutrients and MMC reagents at day 4. Collectively, no further enhancement of fibrillin-1 or fibronectin deposition was observed in lung fibroblasts after 6 d of treatment with Ficoll 70, Ficoll 400 or Ficoll mix, despite an overall increase in fibrillin-1 and fibronectin deposition in untreated controls compared to the prior 4 d untreated cultures (Fig. 2a). Consequently, no significant differences were observed in fluorescence intensity for fibrillin-1 and fibronectin when Ficoll-treated and untreated conditions were compared (Fig. 2b). Likewise, parameters of fibrillin-1 and fibronectin ECM network complexity, such as number of branches and number of junctions, were not significantly changed in Ficoll-treated lung fibroblasts compared to untreated controls after the 7 d culture period (Fig. 2c,d). However, an apparent increase in thickness of

fibrillin-1 fibre bundles across all MMC conditions was observed, which may represent microfibril maturation.

FITC-Ficoll was incorporated into the ECM of lung fibroblasts

To investigate if Ficoll 70 or Ficoll 400 were incorporated into the ECM of lung fibroblasts, lung fibroblasts were treated with FITC-conjugated Ficoll 70, FITC-conjugated Ficoll 400 and FITC-conjugated Ficoll mix. Immunocytochemistry clearly showed the presence of FITC-conjugated Ficoll in the cell layer/ECM of lung fibroblasts after 4 d of culture in all treated conditions (Fig. 3a). Quantification of the relative mean fluorescence intensity originating from the FITC signal confirmed significant FITC-conjugated Ficoll presence in the cell/ECM layer of Ficoll-treated lung fibroblast cultures compared to untreated control cultures (Fig. 3b). Correlating with

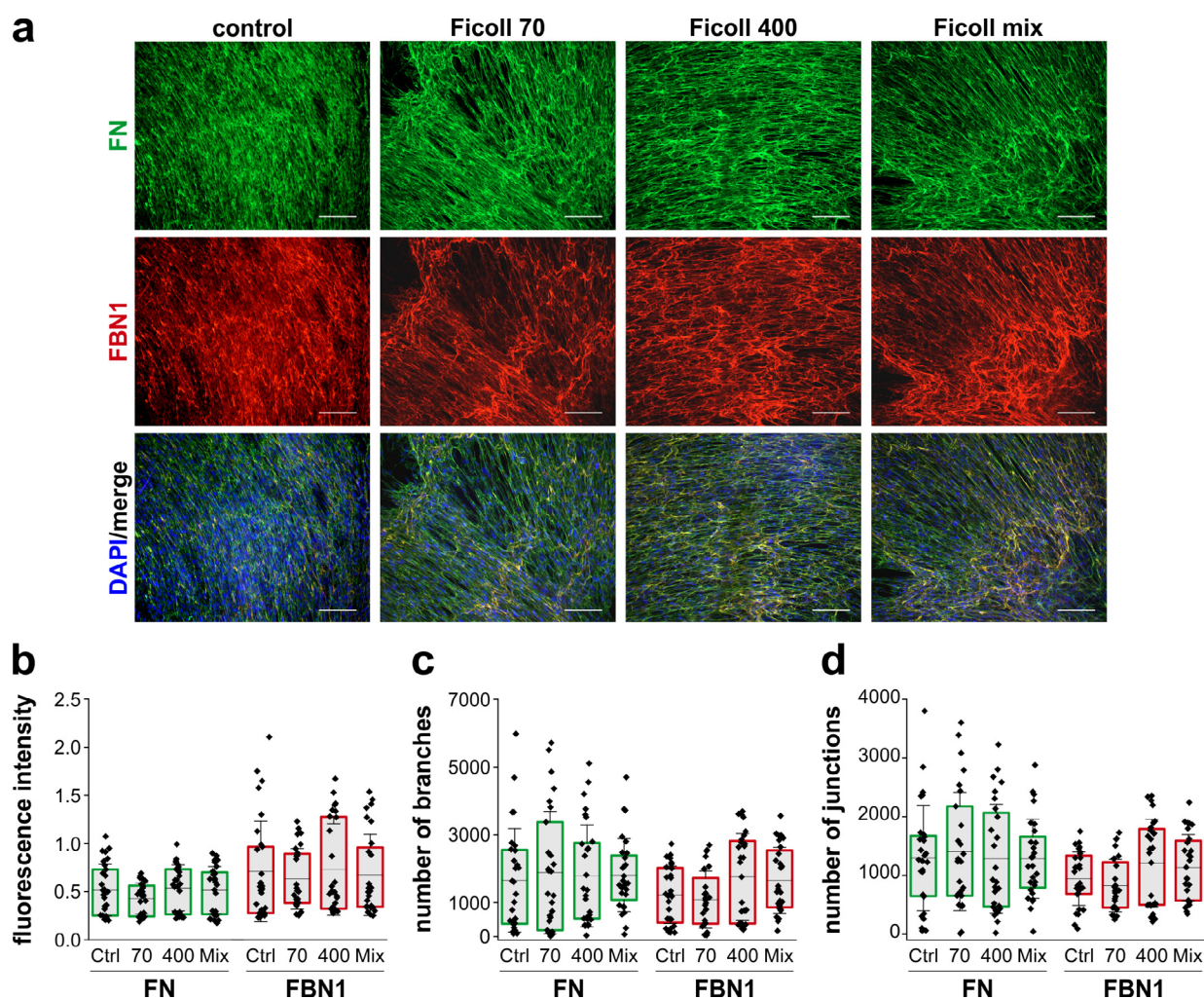


Fig. 2. MMC with Ficoll did not further enhance fibrillin-1 deposition in 7 d cultures. (a) Representative images of indirect immunofluorescence staining for fibronectin (FN) and fibrillin-1 (FBN1) deposited by lung fibroblasts after 6 d in the absence (Ctrl) or presence of Ficoll 70 (70), Ficoll 400 (400) or Ficoll mix (Mix). Nuclei were stained with DAPI. Scale bars = 200 μm. Quantification of (b) fluorescence intensity normalised to DAPI, (c) number of branches and (d) number of junctions. Boxes represent the 25th-75th percentile range and whiskers the standard deviation. Individual data points represent 7-12 fields of view for each condition from $n = 3$ independent experiments. Statistical analysis was performed using a one-way ANOVA followed by *post-hoc* Tukey test. * $p < 0.05$ was considered statistically significant.

the increased fibronectin and fibrillin-1 deposition after Ficoll 400 treatment, a significantly higher ECM deposition was observed in Ficoll 400 compared to Ficoll 70 or Ficoll mix conditions. Notably, while Ficoll 70 and Ficoll 400 could be consistently detected in the cell layer, the levels of Ficoll 400 showed larger inter-experimental variation, suggesting binding to ECM components with varying specificities and, therefore, more variable trapping within nascent ECM. While some of the FITC signal appeared to be more diffusely distributed, FITC-conjugated Ficoll clearly co-stained with fibronectin fibres in the ECM (Fig. 3c,d). Several peaks originating from the FITC signal overlapped with peaks originating from the

fibronectin signal (Fig. 3d, grey arrows). Interestingly, some fibronectin peaks adjacent to those co-stained did not correspond to FITC-conjugated Ficoll 400, again suggesting some specificity and fibre-selective incorporation of FITC-conjugated Ficoll 400 into the ECM (Fig. 3d, black arrows).

MMC with carrageenan promoted aberrant fibrillin-1 and fibronectin deposition

To test if other MMC reagents were able to promote fibrillin-1 deposition, the red seaweed extract carrageenan was added to lung fibroblasts. Carrageenan, in contrast to Ficoll 70 or Ficoll 400, is a negatively charged, polydisperse sulphated

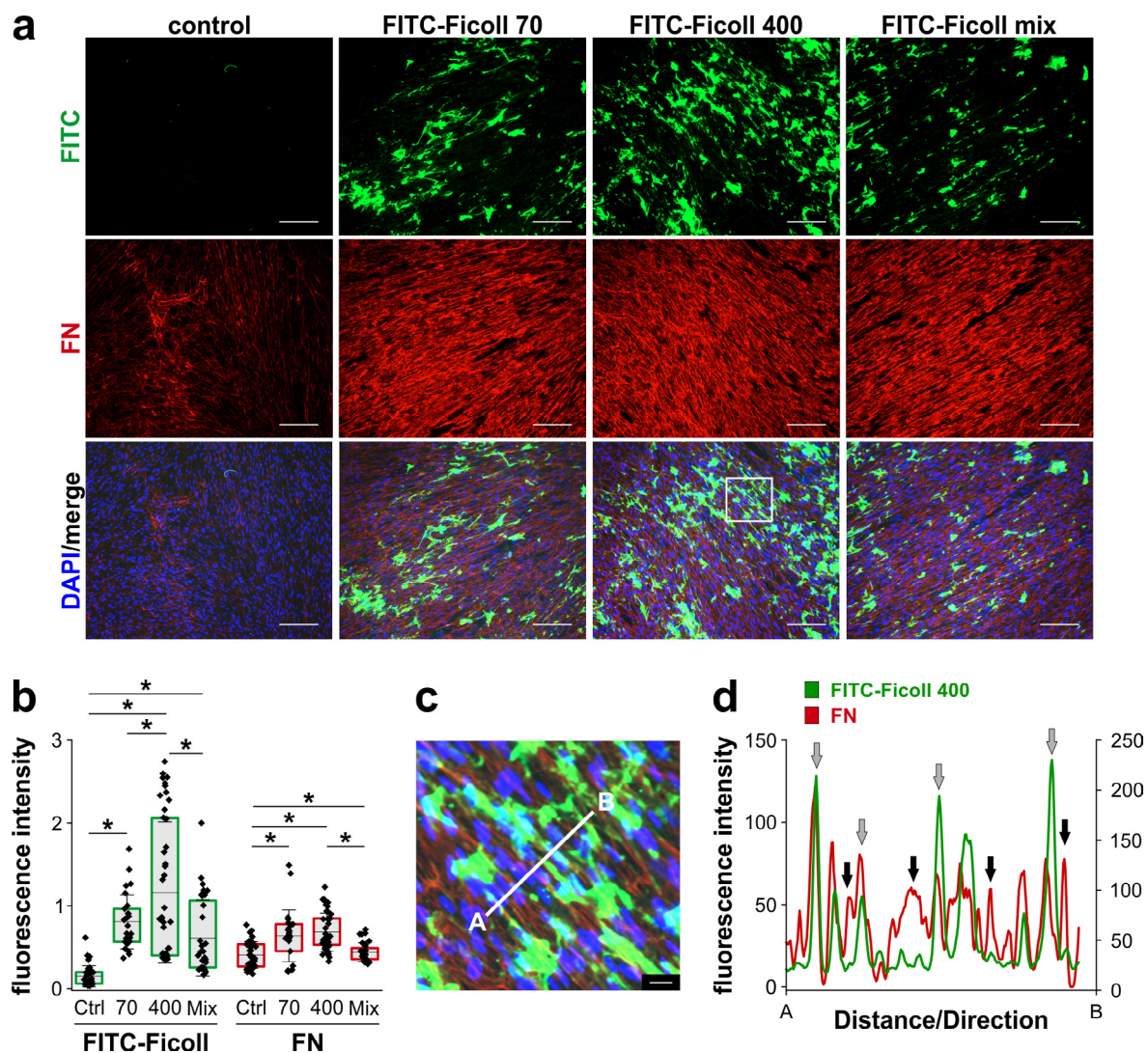


Fig. 3. Ficoll was incorporated into the ECM of lung fibroblasts. (a) Representative images of indirect immunofluorescence staining for fibronectin (FN) and FITC-Ficoll autofluorescence from lung fibroblasts after 3 d in the absence (Ctrl) or presence of FITC-Ficoll 70 (70), FITC-Ficoll 400 (400) or the FITC-Ficoll mix (Mix). Nuclei were stained with DAPI. Scale bars = 200 μ m. White box indicates magnified area in c. (b) Quantification of fluorescence intensity normalised to DAPI. Individual data points represent 5-10 fields of view for each condition from $n = 4$ independent experiments. Boxes represent the 25th-75th percentile range and whiskers the standard deviation. Statistical analysis was performed using a one-way ANOVA followed by *post-hoc* Tukey test. * $p < 0.05$ was considered statistically significant. (c) Digitally magnified image from the white box in a showing the area analysed for co-staining of FN and FITC-Ficoll 400. Scale bar = 20 μ m. (d) Fluorescence intensity profiles representing the red (FN) and green (FITC-Ficoll 400) channels along the white line indicated in c. Profiles were extracted using the BAR script from Fiji/ImageJ.

polysaccharide. Fibrillin-1 and fibronectin deposition were analysed after 4 d and an increase in fibrillin-1 deposition was observed at 50 $\mu\text{g}/\text{mL}$ carrageenan (Fig. 4a,b). However, the ECM deposition pattern was aberrant. Already at 10 $\mu\text{g}/\text{mL}$ carrageenan, globular aggregates of fibrillin-1 were observed, suggesting a disruption in fibrillin-1 ECM deposition without an increase in the total amount of fibrillin-1 (Fig. 4a, insets). At 50 $\mu\text{g}/\text{mL}$, fibrillin-1 was deposited in large aggregates and fibrillin-1 fibres were largely absent. When fibronectin deposition was analysed in the presence of carrageenan, a dose-dependent increase in the normalised fluorescence intensity was found (Fig. 4c,d). However, fibronectin deposition in the presence of carrageenan appeared disorganised,

as patches connected by very fine fibres (Fig. 4c, insets). At 200 $\mu\text{g}/\text{mL}$ carrageenan, a large drop in cell number was observed, suggesting interference with cell proliferation or cell viability (data not shown). Collectively, data suggested that the careful selection of a specific MMC reagent may be required to achieve the optimal desired outcome.

Enhancement of fibrillin-1 deposition in Marfan syndrome patient-derived skin fibroblasts

Since some Marfan syndrome-causing *FBN1* variants can result in reduced ECM deposition of fibrillin-1, it was examined if MMC could promote fibrillin-1 deposition in Marfan syndrome patient-derived skin fibroblasts harbouring either pathogenic nonsense

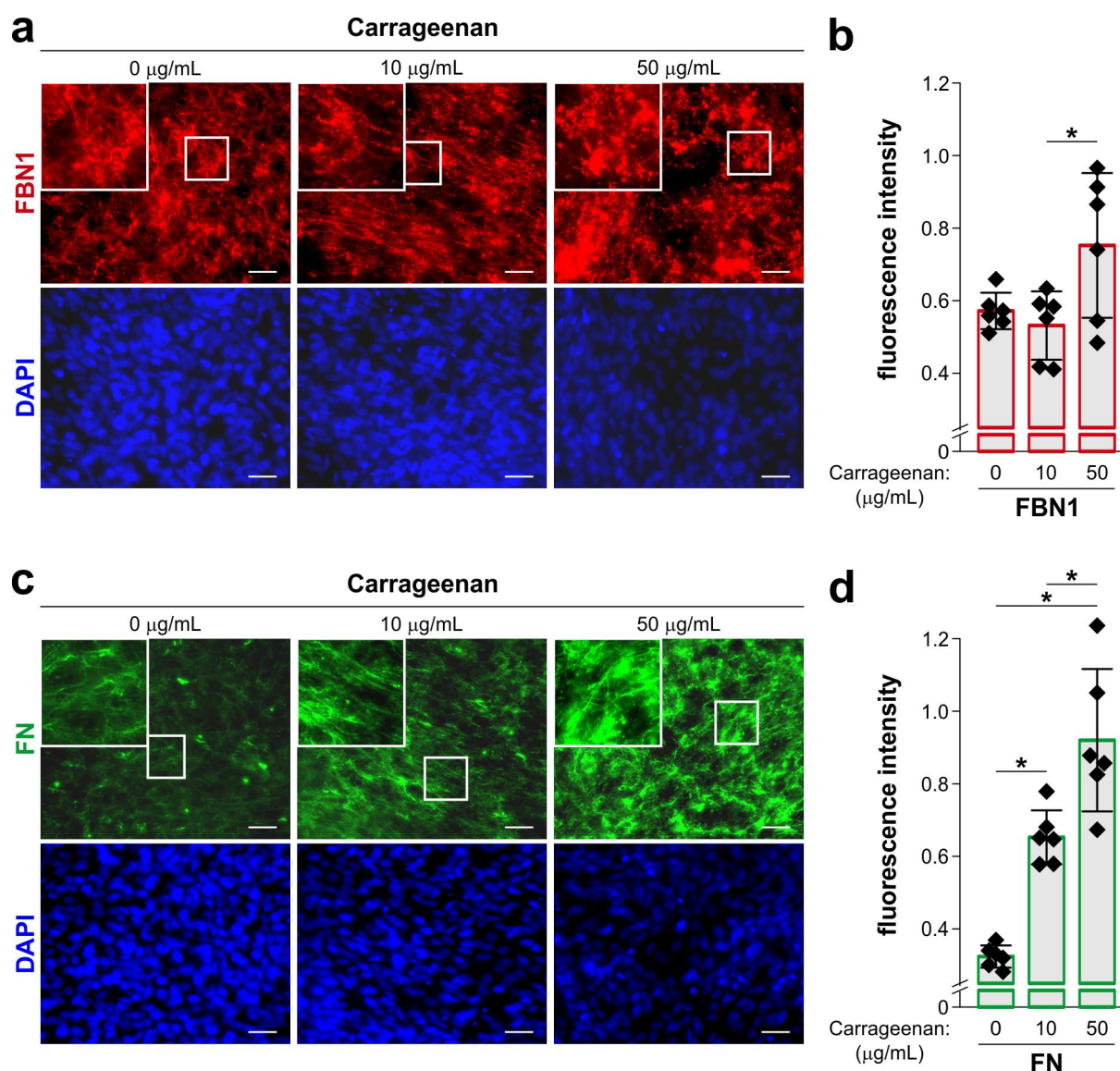


Fig. 4. MMC with carrageenan resulted in aberrant fibrillin-1 deposition. (a) Representative images of indirect immunofluorescence staining for fibrillin-1 (FBN1) deposited by lung fibroblasts after 3 d in the presence of the indicated concentrations of carrageenan. Nuclei were stained with DAPI. Scale bars = 25 μm . (b) Quantification of FBN1 fluorescence intensity normalised to DAPI. (c) Representative images of indirect immunofluorescence staining for fibronectin (FN) deposited by lung fibroblasts after 3 d in the presence of the indicated concentrations of carrageenan. Nuclei were stained with DAPI. Scale bars = 25 μm . (d) Quantification of FN fluorescence intensity normalised to DAPI. Individual data points represent 6 fields of view for each condition from $n = 3$ independent experiments. Statistical analysis was performed using a one-way ANOVA followed by *post-hoc* Tukey test. * $p < 0.05$ was considered statistically significant.

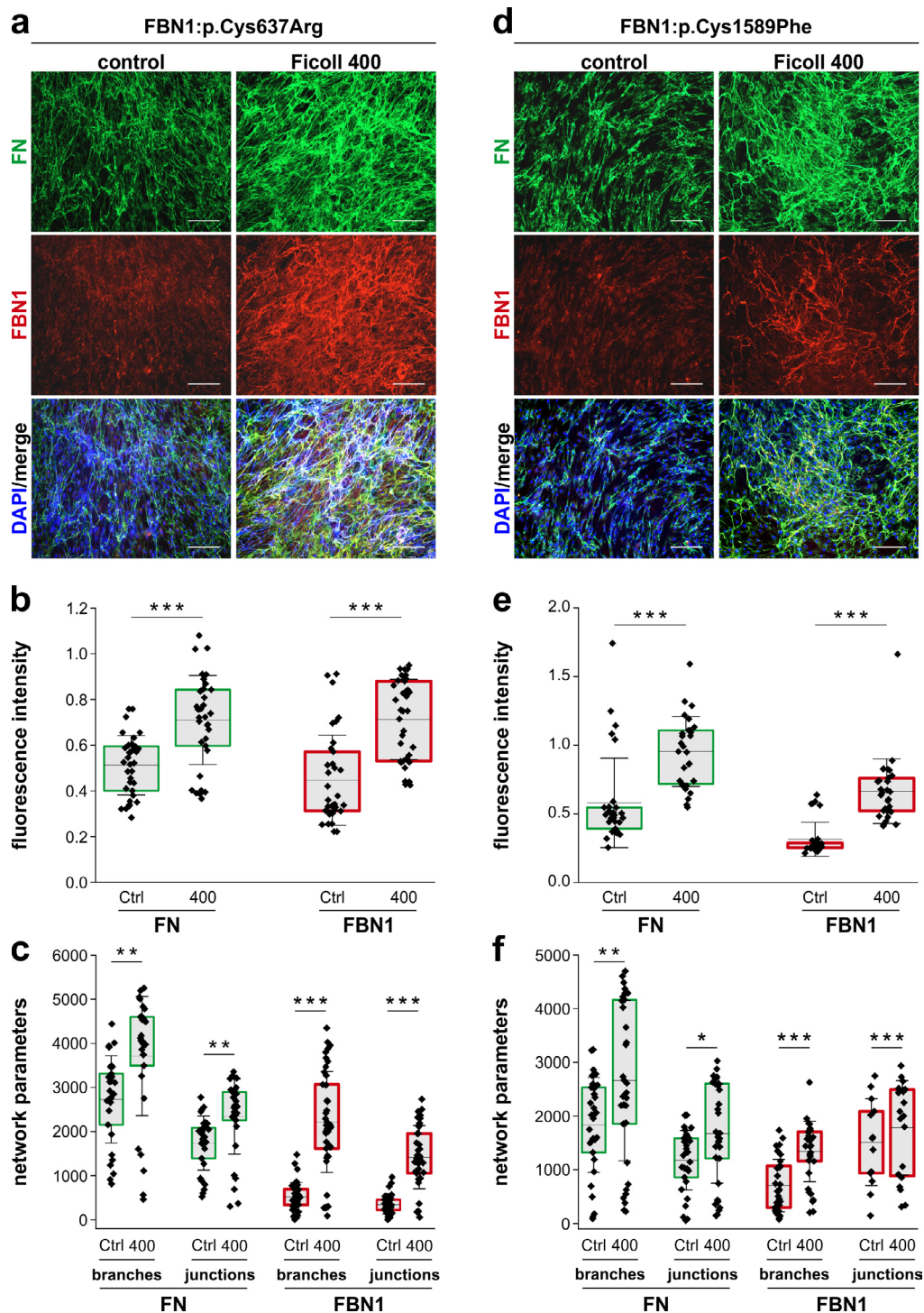


Fig. 5. Enhancement of fibrillin-1 deposition in Marfan syndrome patient-derived fibroblasts FBN1:p.Cys637Arg and FBN1:p.Cys1589Phe. (a) Representative images of indirect immunofluorescence staining for fibronectin (FN) and fibrillin-1 (FBN1) deposited by FBN1:p.Cys637Arg fibroblasts after 3 d in the presence (400) or absence (Ctrl) of Ficoll 400. Nuclei were stained with DAPI. Scale bars = 200 μ m. (b) Quantification of FN and FBN1 fluorescence intensity normalised to DAPI. (c) Number of branches and number of junctions in the FN and FBN1 ECM networks. Individual data points represent 4-13 fields of view for each condition from $n = 4$ independent experiments. Boxes represent the 25th-75th percentile range and whiskers the standard deviation. (d) Representative images of indirect immunofluorescence staining for FN and FBN1 deposited by FBN1:p.Cys1589Phe fibroblasts after 3 d in the presence or absence of Ficoll 400. Nuclei were stained with DAPI. Scale bars = 200 μ m. (e) Quantification of FN and FBN1 fluorescence intensity normalised to DAPI. (f) Number of branches and number of junctions in the FN and FBN1 ECM networks. Individual data points represent 5-13 fields of view for each condition from $n = 3$ independent experiments. Boxes represent the 25th-75th percentile range and whiskers the standard deviation. Statistical analysis was performed using a two-sample Student's *t*-test. A $p < 0.05$ was considered statistically significant. * $p < 0.05$, ** $p < 0.01$, *** $p < 0.001$.

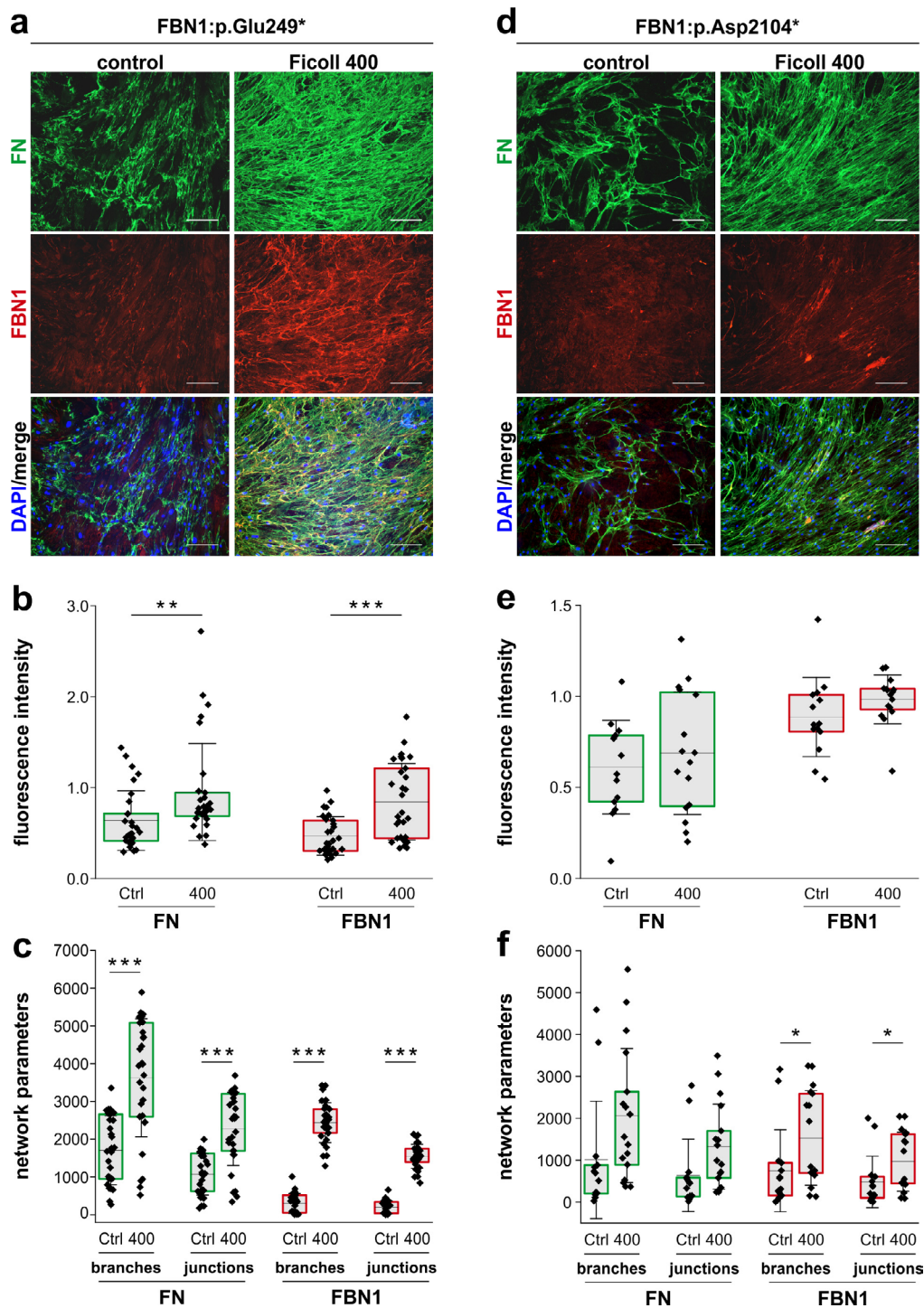


Fig. 6. Enhancement of fibrillin-1 deposition in Marfan syndrome patient-derived fibroblasts FBN1:p.Glu249* and FBN1:p.Asp2104*. (a) Representative images of indirect immunofluorescence staining for fibronectin (FN) and fibrillin-1 (FBN1) deposited by FBN1:p.Glu249* fibroblasts after 3 d in the presence (400) or absence (Ctrl) of Ficoll 400. Nuclei were stained with DAPI. Scale bars = 200 μ m. (b) Quantification of FN and FBN1 fluorescence intensity normalised to DAPI. (c) Number of branches and number of junctions in the FN and FBN1 ECM networks. Individual data points represent 3-13 fields of view per condition from $n = 3$ independent experiments. Boxes represent the 25th-75th percentile range and whiskers the standard deviation. (d) Representative images of indirect immunofluorescence staining for FN and FBN1 deposited by FBN1:p.Asp2104* fibroblasts after 3 d in the presence or absence of Ficoll 400. Nuclei were stained with DAPI. Scale bars = 200 μ m. (e) Quantification of FN and FBN1 fluorescence intensity normalised to DAPI. (f) Number of branches and number of junctions in the FN and FBN1 ECM networks. Individual data points represent 3-7 fields of view for each condition from $n = 3$ independent experiments. Boxes represent the 25th-75th percentile range and whiskers the standard deviation. Statistical analysis was performed using a two-sample Student's *t*-test. A $p < 0.05$ was considered statistically significant. * $p < 0.05$, ** $p < 0.01$, *** $p < 0.001$.

variants in *FBN1*, resulting in premature termination codons, or missense variants, altering the primary fibrillin-1 amino acid sequence (Aoyama *et al.*, 1994; Milewicz *et al.*, 1992). 4 cell lines of primary dermal fibroblasts derived from Marfan syndrome patients were chosen for treatment with Ficoll 400 (Table 1). 2 of the cell lines contained missense variants in *FBN1* (FBN1:p.Cys637Arg, FBN1:p.Cys1589Phe) while the other 2 contained nonsense variants (FBN1:p.Glu249*, FBN1:p.Asp2104*) (Schrijver *et al.*, 1999; Schrijver *et al.*, 2002; Tynan *et al.*, 1993). Fibronectin and fibrillin-1 deposition were visualised by immunocytochemistry after 4 d of culture, *i.e.* 3 d of Ficoll 400 treatment. 3 of the 4 Marfan patient-derived cell lines showed variable, but significant, enhancement of fibronectin and fibrillin-1 deposition after treatment with Ficoll 400, compared to untreated controls. Of the 2 cell lines harbouring missense variants, fibrillin-1 ECM deposition showed more enhancement in the cell line harbouring the FBN1:p.Cys637Arg variant when compared to the line harbouring the FBN1:p.Cys1589Phe variant (Fig. 5a,d). However, increases in fluorescence intensity and changes in ECM network parameters were significant for fibronectin and fibrillin-1 in both cell lines (Fig. 5b,c,e,f). Of the 2 cell lines harbouring *FBN1* nonsense variants, fibrillin-1 showed increased deposition in the presence of Ficoll 400 in FBN1:p.Glu249* cells only (Fig. 6a). Fluorescence signal intensity and changes in network parameters indicated increased ECM deposition and denser ECM networks (Fig. 6b,c). In contrast, fibrillin-1 deposition in FBN1:p.Asp2104* cells, which also harboured a premature termination codon in *FBN1*, did not respond to Ficoll 400 treatment (Fig. 6d). Changes in fluorescence signal intensities for fibronectin and fibrillin-1 were not significant (Fig. 6e). Network parameters for the fibrillin-1 network, but not the fibronectin network, did show significant changes, albeit with smaller fold changes than were observed for the other 3 cell lines (Fig. 6f). Collectively, the response of Marfan syndrome patient-derived skin fibroblasts to Ficoll 400 treatment showed cell line-dependent changes in overall fibronectin and fibrillin-1 deposition, which were largely reflected by changes in the fibronectin and fibrillin-1 ECM network parameters.

Discussion

The present study showed that MMC can promote the deposition of a critical ECM scaffolding protein, fibrillin-1, in a human lung fibroblast cell line as well as in several Marfan syndrome patient-derived skin fibroblasts. Since fibrillin-1 microfibrils are required for the formation and maintenance of elastic fibres and for the deposition of LTBP3 and fibulins as well as TGF β and BMP growth factors, these findings could be broadly relevant for tissue-engineering approaches to generate elastic tissues, such as blood

vessels, tendons or skin (Ramirez and Rifkin, 2009; Zimmermann *et al.*, 2021). In addition, findings supported the notion that biochemical processes, such as ECM formation, may be accelerated by MMC in cell culture settings, which may better represent the highly concentrated, *i.e.* crowded, cellular microenvironments *in vivo* (Tsiapalis and Zeugolis, 2021).

The capability of MMC to enhance ECM deposition over time has been previously shown for fibronectin and collagen types I, III, IV, V and VI (Chen *et al.*, 2013; Chen *et al.*, 2011; Graham *et al.*, 2019; Tsiapalis *et al.*, 2020). These ECM proteins are key components of a diverse range of connective tissues, including tendon, cartilage, blood vessels and skeletal muscle. For fibrillin-1, MMC promoted its ECM deposition with significant differences after 4 d but not after 7 d in culture. The high efficacy of MMC at 4 d suggested an immediacy in the crowding effect, possibly due to increased absolute concentrations of fibrillin-1 or increased cell surface concentrations of fibrillin-1 assembly mediators, such as heparan sulphate proteoglycans or fibronectin (Sabatier *et al.*, 2009; Tiedemann *et al.*, 2001). In addition, biochemical processes, such as fibrillin-1 multimerisation, fibrillin-1 N-to-C-terminal self-interactions or furin processing of N- and C-terminal pro-peptides could be promoted to accelerate the deposition of fibrillin-1 microfibrils (Hubmacher *et al.*, 2008; Jensen *et al.*, 2014; Lin *et al.*, 2002; Raghunath *et al.*, 1999). In support, expedited collagen pro-peptide processing was previously shown in the presence of MMC reagents (Lareu *et al.*, 2007). Western blot data also suggested increased fibrillin-1 deposition, as fibrillin-1 protein was consistently reduced in the medium in the presence of Ficoll. However, the decreased disparity at 7 d suggested a maximum capacity for fibrillin-1 ECM deposition, which could be limited by reaching the capacity of cell surface receptors or by steric hindrance. Alternatively, the observed presence of Ficoll in the pericellular matrix or ECM may limit the amount of ECM that can be deposited. Ficoll could also bind to and interfere with the ECM formational function of ECM proteins, such as cell surface receptors, perlecan or heparan sulphate proteoglycans. In that case, Ficoll may not be entirely inert and could thus interfere with ECM assembly processes in a protein-specific manner. Using collagen deposition as a model, it was indeed shown that addition of the MMC reagent dextran sulphate, which is anionic in nature, worked not only through volume exclusion, but also promoted collagen deposition through additional mechanisms (Lareu *et al.*, 2007). The preferential MMC enhancement of fibrillin-1 deposition with Ficoll 400 may contradict prior literature observing optimal ECM deposition with a 60:40 (w/w) Ficoll mix and no enhancement when Ficoll 70 or Ficoll 400 were used individually. Since these studies investigated predominantly deposition of various collagens, differences in the mechanisms of collagen *versus* fibrillin-1 deposition

could explain the different results. This would suggest that MMC as a process has distinct consequences for individual ECM proteins, depending upon the specific MMC reagent used and the cell or tissue context. Carrageenan, a representative charged MMC reagent, while increasing fibrillin-1 and fibronectin deposition, profoundly altered their deposition pattern in the ECM. Therefore, several biophysically different MMC reagents may need to be screened to achieve the maximum intended output for the specific target protein or biochemical process, and multiple parameters, such as increases in the amount of target protein, appropriate organisation in the ECM, functional assays and changes in cell behaviour may warrant consideration.

The analysis of MMC in the context of fibrillin-1 deposition in Marfan syndrome patient-derived skin fibroblasts offered insights into the efficacy of MMC in cases of ECM protein dysfunction. Notably, fibrillin-1 deposition can be impaired due to pathogenic variants in *FBN1* (Aoyama *et al.*, 1994; Milewicz *et al.*, 1992). Of the 4 Marfan syndrome patient-derived fibroblast lines, 3 showed significant enhancement in fibrillin-1 deposition in the ECM after treatment with Ficoll 400. The disparity in the responses of these fibroblasts to MMC is notable though unsurprising given that the > 1,800 individual *FBN1* variants in patients with Marfan syndrome can be categorised into 5 groups based upon biochemical consequences (Aoyama *et al.*, 1994; Collod-Beroud *et al.*, 2003). The first 2 groups of *FBN1* variants resulted in reduced deposition but normal secretion. The third and fourth groups showed normal fibrillin-1 synthesis but either mildly or severely impaired fibrillin-1 ECM deposition. The fifth group shows normal fibrillin-1 synthesis, secretion and ECM deposition. Data suggested that both Marfan syndrome patient-derived fibroblasts harbouring nonsense and missense variants showed responsive fibrillin-1 increase with addition of Ficoll 400. However, higher fibrillin-1 deposition enhancement in fibroblasts harbouring missense variants could be explained by more fibrillin production in these cell lines, if the mutant fibrillin-1 protein does not exert a dominant negative effect, *i.e.* interferes with the deposition of wild type fibrillin-1. Alternatively, factors such as age at sampling, individual genetic background, passage number and other patient-specific circumstances could influence the response of these cells to MMC. One interesting example is the subset of *FBN1* variants causing neonatal Marfan syndrome, the most severe form of Marfan syndrome, where patients typically die within the first year of life due to congestive heart failure. In these cases, fibrillin-1 deposition of patient-derived fibroblasts was not only reduced, as is the case in many fibroblasts from patients with classical Marfan syndrome, but also the quality of the fibrillin-1 microfibrils was altered. Microfibrils were described as thin, frayed and fragmented; fibrillin-1 deposits in

the ECM appeared stippled or as globular aggregates (Godfrey *et al.*, 1995; Hanseus *et al.*, 1995; Karttunen *et al.*, 1994; Lonnqvist *et al.*, 1996; Milewicz and Duvic, 1994; Raghunath *et al.*, 1993; Superti-Furga *et al.*, 1992; Wang *et al.*, 1995). In several instances, no fibrillin-1 microfibrils were produced by hyperconfluent patient-derived skin fibroblasts (Karttunen *et al.*, 1994; Lonnqvist *et al.*, 1996; Wang *et al.*, 1995). It would be interesting to test experimentally if MMC could restore fibrillin-1 deposition towards a more classical pattern, with a less fragmented fibrillin-1 microfibril network, or if it would exacerbate the observed phenotypes. A more recent study showed that recombinant full-length FBN1 harbouring neonatal Marfan syndrome variants does not incorporate into fibrillin-1 microfibrils, which suggests the latter (Jensen *et al.*, 2021).

From a clinical perspective, it is highly unlikely that MMC will be developed into a treatment modality for Marfan syndrome. The most likely applications of MMC within a fibrillin-1 context are in basic research, to better understand the formation of fibrillin-1 microfibrils and the hierarchical assembly of microfibril-associated proteins in the ECM, and in tissue-engineering approaches to rebuild elastic tissues such as skin, tendon or large blood vessels. Tissue engineering for regeneration or repair specifically requires biomimicry of the assembled tissue and a fidelity in the assembled constructs to accurately model *in vivo* function. Accordingly, these methods often depend on self-assembly of endogenous ECM molecules to construct supramolecular assemblies with repeatable precision, ideally using autologous host or patient-derived cells. MMC allows for secreted biomolecules to interact more effectively or efficiently with naturally produced, tissue-specific ECM to compose a more emulative implantable construct. Thus, a key motivation in the study and application of MMC is its capacity to augment bioengineering strategies by shortening cell culture and incubation times in order to limit cellular senescence, phenotypic drift of cell types when using undifferentiated stem cells and unwanted epigenetic modifications, which all can arise as a result of the extended culture times currently required for engineering cell-derived tissue repair constructs (Lee *et al.*, 2016; Peng *et al.*, 2012; Shendi *et al.*, 2019). In addition, Ficoll 400 or other MMC reagents could be integrated in engineered tissue grafts to promote fibrillin-1 and other ECM protein deposition from endogenous cells after they repopulate the graft material (Satyam *et al.*, 2014).

In summary, the present study demonstrated enhancement of fibrillin-1 and fibronectin deposition in the presence of MMC reagents in lung fibroblasts, underscoring the potency of MMC to generate a more extensive ECM in shorter time periods but also demonstrating the need for careful MMC reagent selection to avoid aberrant ECM deposition of target molecules. The potential to increase fibrillin-1

ECM deposition suggested possible applications in tissue engineering and basic research. Moreover, it illustrated the potency of MMC in cell culture systems to better approximate biological ECM environments when studying interactions of ECM proteins, such as fibrillin-1 or fibronectin. Thus, MMC may serve not only as a logical next step in the quest for cell culture innovation but as a forward path for *in vitro* reproduction of cell function in healthy biological tissues.

Acknowledgements

This study was supported by seed funding from the Leni & Peter W. May Department of Orthopaedics (Icahn School of Medicine at Mount Sinai) and, in part, by funding from the National Institutes of Health (AR070748 to D.H.) We are grateful to Dr Dieter Reinhardt (McGill University, Montreal, Canada) for generously providing the fibrillin-1 antibody.

References

- Aoyama T, Francke U, Dietz HC, Furthmayr H (1994) Quantitative differences in biosynthesis and extracellular deposition of fibrillin in cultured fibroblasts distinguish five groups of Marfan syndrome patients and suggest distinct pathogenetic mechanisms. *J Clin Invest* **94**: 130-137.
- Balic Z, Misra S, Willard B, Reinhardt DP, Apte SS, Hubmacher D (2021) Alternative splicing of the metalloprotease ADAMTS17 spacer regulates secretion and modulates autolytic activity. *FASEB J* **35**: e21310. DOI: 10.1096/fj.202001120RR.
- Chen B, Wang B, Zhang WJ, Zhou G, Cao Y, Liu W (2013) Macromolecular crowding effect on cartilaginous matrix production: a comparison of two-dimensional and three-dimensional models. *Tissue Eng Part C Methods* **19**: 586-595.
- Chen C, Loe F, Blocki A, Peng Y, Raghunath M (2011) Applying macromolecular crowding to enhance extracellular matrix deposition and its remodeling *in vitro* for tissue engineering and cell-based therapies. *Adv Drug Deliv Rev* **63**: 277-290.
- Collod-Beroud G, Le Bourdelles S, Ades L, Ala-Kokko L, Booms P, Boxer M, Child A, Comeglio P, De Paepe A, Hyland JC, Holman K, Kaitila I, Loeys B, Matyas G, Nuytinck L, Peltonen L, Rantamaki T, Robinson P, Steinmann B, Junien C, Beroud C, Boileau C (2003) Update of the UMD-FBN1 mutation database and creation of an FBN1 polymorphism database. *Hum Mutat* **22**: 199-208.
- De Pieri A, Rana S, Korntner S, Zeugolis DI (2020) Seaweed polysaccharides as macromolecular crowding agents. *Int J Biol Macromol* **164**: 434-446.
- Dietz HC, Cutting GR, Pyeritz RE, Maslen CL, Sakai LY, Corson GM, Puffenberger EG, Hamosh A, Nanthakumar EJ, Curristin SM, *et al.* (1991) Marfan syndrome caused by a recurrent de novo missense mutation in the fibrillin gene. *Nature* **352**: 337-339.
- El-Hallous E, Sasaki T, Hubmacher D, Getie M, Tiedemann K, Brinckmann J, Batge B, Davis EC, Reinhardt DP (2007) Fibrillin-1 interactions with fibulins depend on the first hybrid domain and provide an adaptor function to tropoelastin. *J Biol Chem* **282**: 8935-8946.
- Ellis RJ (2001) Macromolecular crowding: obvious but underappreciated. *Trends Biochem Sci* **26**: 597-604.
- Faivre L, Gorlin RJ, Wirtz MK, Godfrey M, Dagoneau N, Samples JR, Le Merrer M, Collod-Beroud G, Boileau C, Munnich A, Cormier-Daire V (2003) In frame fibrillin-1 gene deletion in autosomal dominant Weill-Marchesani syndrome. *J Med Genet* **40**: 34-36.
- Garnica-Galvez S, Korntner SH, Skoufos I, Tzora A, Diakakis N, Prassinou N, Zeugolis DI (2021) Hyaluronic acid as macromolecular crowder in equine adipose-derived stem cell cultures. *Cells* **10**: 859. DOI: 10.3390/cells10040859.
- Gaspar D, Fuller KP, Zeugolis DI (2019) Polydispersity and negative charge are key modulators of extracellular matrix deposition under macromolecular crowding conditions. *Acta Biomater* **88**: 197-210.
- Godfrey M, Raghunath M, Cisler J, Bevins CL, DePaepe A, Di Rocco M, Gregoritch J, Imaizumi K, Kaplan P, Kuroki Y, Silberbach M, Superti-Furga A, Van Thienen M-N, Vetter U, Steinmann B (1995) Abnormal morphology of fibrillin microfibrils in fibroblast cultures from patients with neonatal Marfan syndrome. *Am J Pathol* **146**: 1414-1421.
- Graham J, Raghunath M, Vogel V (2019) Fibrillar fibronectin plays a key role as nucleator of collagen I polymerization during macromolecular crowding-enhanced matrix assembly. *Biomater Sci* **7**: 4519-4535.
- Hanseus K, Lundberg LM, Bjorkhem G, Dahlback K, Hagerstrand I, Kristoffersson U (1995) Clinical and immunohistochemical findings in a case of neonatal Marfan syndrome. *Acta Paediatr* **84**: 1329-1332.
- Hubmacher D, El-Hallous EI, Nelea V, Kaartinen MT, Lee ER, Reinhardt DP (2008) Biogenesis of extracellular microfibrils: multimerization of the fibrillin-1 C terminus into bead-like structures enables self-assembly. *Proc Natl Acad Sci U S A* **105**: 6548-6553.
- Hubmacher D, Tiedemann K, Bartels R, Brinckmann J, Vollbrandt T, Batge B, Notbohm H, Reinhardt DP (2005) Modification of the structure and function of fibrillin-1 by homocysteine suggests a potential pathogenetic mechanism in homocystinuria. *J Biol Chem* **280**: 34946-34955.
- Jensen SA, Aspinall G, Handford PA (2014) C-terminal propeptide is required for fibrillin-1 secretion and blocks premature assembly through linkage to domains cbEGF41-43. *Proc Natl Acad Sci U S A* **111**: 10155-10160.
- Jensen SA, Atwa O, Handford PA (2021) Assembly assay identifies a critical region of human fibrillin-1

required for 10-12 nm diameter microfibril biogenesis. *PLoS One* **16**: e0248532. DOI: 10.1371/journal.pone.0248532.

Karamanos NK, Theocharis AD, Piperigkou Z, Manou D, Passi A, Skandalis SS, Vynios DH, Oriant-Rousseau V, Ricard-Blum S, Schmelzer CEH, Duca L, Durbeek M, Afratis NA, Troeberg L, Franchi M, Masola V, Onisto M (2021) A guide to the composition and functions of the extracellular matrix. *The FEBS J* **28**: 6850-6912.

Karttunen L, Raghunath M, Lonnqvist L, Peltonen L (1994) A compound-heterozygous Marfan patient: two defective fibrillin alleles result in a lethal phenotype. *Am J Hum Genet* **55**: 1083-1091.

Kumar P, Satyam A, Fan X, Collin E, Rochev Y, Rodriguez BJ, Gorelov A, Dillon S, Joshi L, Raghunath M, Pandit A, Zeugolis DI (2015) Macromolecularly crowded *in vitro* microenvironments accelerate the production of extracellular matrix-rich supramolecular assemblies. *Sci Rep* **5**: 8729. DOI: 10.1038/srep08729.

Kumra H, Nelea V, Hakami H, Pagliuzza A, Djokic J, Xu J, Yanagisawa H, Reinhardt DP (2019) Fibulin-4 exerts a dual role in LTBP-4L-mediated matrix assembly and function. *Proc Natl Acad Sci U S A* **116**: 20428-20437.

Lareu RR, Subramhanya KH, Peng Y, Benny P, Chen C, Wang Z, Rajagopalan R, Raghunath M (2007) Collagen matrix deposition is dramatically enhanced *in vitro* when crowded with charged macromolecules: the biological relevance of the excluded volume effect. *FEBS Lett* **581**: 2709-2714.

Laurent TC (1963) The interaction between polysaccharides and other macromolecules. 5. The solubility of proteins in the presence of dextran. *Biochem J* **89**: 253-257.

Le Goff C, Mahaut C, Wang LW, Allali S, Abhyankar A, Jensen S, Zylberberg L, Collod-Beroud G, Bonnet D, Alanay Y, Brady AF, Cordier MP, Devriendt K, Genevieve D, Kiper PO, Kitoh H, Krakow D, Lynch SA, Le Merrer M, Megarbane A, Mortier G, Odent S, Polak M, Rohrbach M, Sillence D, Stolte-Dijkstra I, Superti-Furga A, Rimoin DL, Topouchian V, Unger S, Zabel B, Bole-Feysot C, Nitschke P, Handford P, Casanova JL, Boileau C, Apte SS, Munnich A, Cormier-Daire V (2011) Mutations in the TGFbeta binding-protein-like domain 5 of FBN1 are responsible for acromicric and geleophysic dysplasias. *Am J Hum Genet* **89**: 7-14.

Lee MH, Goralczyk AG, Kriszt R, Ang XM, Badowski C, Li Y, Summers SA, Toh SA, Yassin MS, Shabbir A, Sheppard A, Raghunath M (2016) ECM microenvironment unlocks brown adipogenic potential of adult human bone marrow-derived MSCs. *Sci Rep* **6**: 21173. DOI: 10.1038/srep21173.

Lin G, Tiedemann K, Vollbrandt T, Peters H, Batge B, Brinckmann J, Reinhardt DP (2002) Homo- and heterotypic fibrillin-1 and -2 interactions constitute the basis for the assembly of microfibrils. *J Biol Chem* **277**: 50795-50804.

Lonnqvist L, Karttunen L, Rantamaki T, Kielty C, Raghunath M, Peltonen L (1996) A point mutation creating an extra N-glycosylation site in fibrillin-1 results in neonatal Marfan syndrome. *Genomics* **36**: 468-475.

Mecham RP, Heuser J (1990) Three-dimensional organization of extracellular matrix in elastic cartilage as viewed by quick freeze, deep etch electron microscopy. *Connect Tissue Res* **24**: 83-93.

Milewicz DM, Duvic M (1994) Severe neonatal Marfan syndrome resulting from a *de novo* 3-bp insertion into the fibrillin gene on chromosome 15. *Am J Hum Genet* **54**: 447-453.

Milewicz DM, Pyeritz RE, Crawford ES, Byers PH (1992) Marfan syndrome: defective synthesis, secretion, and extracellular matrix formation of fibrillin by cultured dermal fibroblasts. *J Clin Invest* **89**: 79-86.

Ogston AG, Phelps CF (1960) Exclusion of inulin from solutions of hyaluronic acid. *Nature* **187**: 1024. DOI: 10.1038/1871024a0.

Ogston AG, Phelps CF (1961) The partition of solutes between buffer solutions and solutions containing hyaluronic acid. *Biochem J* **78**: 827-833.

Peng Y, Bocker MT, Holm J, Toh WS, Hughes CS, Kidwai F, Lajoie GA, Cao T, Lyko F, Raghunath M (2012) Human fibroblast matrices bio-assembled under macromolecular crowding support stable propagation of human embryonic stem cells. *J Tissue Eng Regen Med* **6**: e74-86.

Raghunath M, Putnam EA, Ritty T, Hamstra D, Park ES, Tschodrich-Rotter M, Peters R, Rehemtulla A, Milewicz DM (1999) Carboxy-terminal conversion of profibrillin to fibrillin at a basic site by PACE/furin-like activity required for incorporation in the matrix. *J Cell Sci* **112 (Pt 7)**: 1093-1100.

Raghunath M, Superti-Furga A, Godfrey M, Steinmann B (1993) Decreased extracellular deposition of fibrillin and decorin in neonatal Marfan syndrome fibroblasts. *Hum Genet* **90**: 511-515.

Ramirez F, Rifkin DB (2009) Extracellular microfibrils: contextual platforms for TGFbeta and BMP signaling. *Curr Opin Cell Biol* **21**: 616-622.

Rivas G, Minton AP (2016) Macromolecular crowding *in vitro*, *in vivo*, and in between. *Trends Biochem Sci* **41**: 970-981.

Sabatier L, Chen D, Fagotto-Kaufmann C, Hubmacher D, McKee MD, Annis DS, Mosher DF, Reinhardt DP (2009) Fibrillin assembly requires fibronectin. *Mol Biol Cell* **20**: 846-858.

Satyam A, Subramanian GS, Raghunath M, Pandit A, Zeugolis DI (2014) *In vitro* evaluation of Ficoll-enriched and genipin-stabilised collagen scaffolds. *J Tissue Eng Regen Med* **8**: 233-241.

Schindelin J, Arganda-Carreras I, Frise E, Kaynig V, Longair M, Pietzsch T, Preibisch S, Rueden C, Saalfeld S, Schmid B, Tinevez JY, White DJ, Hartenstein V, Eliceiri K, Tomancak P, Cardona A (2012) Fiji: an open-source platform for biological-image analysis. *Nat Methods* **9**: 676-682.

Schrijver I, Liu W, Brenn T, Furthmayr H, Francke U (1999) Cysteine substitutions in epidermal growth factor-like domains of fibrillin-1: distinct effects on biochemical and clinical phenotypes. *Am J Hum Genet* **65**: 1007-1020.

Schrijver I, Liu W, Odom R, Brenn T, Oefner P, Furthmayr H, Francke U (2002) Premature termination mutations in FBN1: distinct effects on differential allelic expression and on protein and clinical phenotypes. *Am J Hum Genet* **71**: 223-237.

Sengle G, Charbonneau NL, Ono RN, Sasaki T, Alvarez J, Keene DR, Bachinger HP, Sakai LY (2008) Targeting of bone morphogenetic protein growth factor complexes to fibrillin. *J Biol Chem* **283**: 13874-13888.

Shendi D, Marzi J, Linthicum W, Rickards AJ, Dolivo DM, Keller S, Kauss MA, Wen Q, McDevitt TC, Dominko T, Schenke-Layland K, Rolle MW (2019) Hyaluronic acid as a macromolecular crowding agent for production of cell-derived matrices. *Acta Biomater* **100**: 292-305.

Stanley S, Balic Z, Hubmacher D (2020) Acromelic dysplasias: how rare musculoskeletal disorders reveal biological functions of extracellular matrix proteins. *Ann N Y Acad Sci* **1490**: 57-76.

Superti-Furga A, Raghunath M, Willems PJ (1992) Deficiencies of fibrillin and decorin in fibroblast cultures of a patient with neonatal Marfan syndrome. *J Med Genet* **29**: 875-878.

Taye N, Karoulias SZ, Hubmacher D (2020) The "other" 15-40%: the role of non-collagenous extracellular matrix proteins and minor collagens in tendon. *J Orthop Res* **38**: 23-35.

Theocharis AD, Manou D, Karamanos NK (2019) The extracellular matrix as a multitasking player in disease. *FEBS J* **286**: 2830-2869.

Tiedemann K, Batge B, Muller PK, Reinhardt DP (2001) Interactions of fibrillin-1 with heparin/heparan sulfate, implications for microfibrillar assembly. *J Biol Chem* **276**: 36035-36042.

Tsiapalis D, De Pieri A, Spanoudes K, Sallent I, Kearns S, Kelly JL, Raghunath M, Zeugolis DI (2020) The synergistic effect of low oxygen tension and macromolecular crowding in the development of extracellular matrix-rich tendon equivalents. *Biofabrication* **12**: 025018. DOI: 10.1088/1758-5090/ab6412.

Tsiapalis D, Zeugolis DI (2021) It is time to crowd your cell culture media – physicochemical considerations with biological consequences. *Biomaterials* **275**: 120943. DOI: 10.1016/j.biomaterials.2021.120943.

Tynan K, Comeau K, Pearson M, Wilgenbus P, Levitt D, Gasner C, Berg MA, Miller DC, Francke U (1993) Mutation screening of complete fibrillin-1 coding sequence: report of five new mutations, including two in 8-cysteine domains. *Hum Mol Genet* **2**: 1813-1821.

Wang M, Price C, Han J, Cisler J, Imaizumi K, Van Thienen MN, DePaepe A, Godfrey M (1995) Recurrent

mis-splicing of fibrillin exon 32 in two patients with neonatal Marfan syndrome. *Hum Mol Genet* **4**: 607-613.

Zeiger AS, Loe FC, Li R, Raghunath M, Van Vliet KJ (2012) Macromolecular crowding directs extracellular matrix organization and mesenchymal stem cell behavior. *PLoS One* **7**: e37904. DOI: 10.1371/journal.pone.0037904.

Zeugolis DI (2021) Bioinspired *in vitro* microenvironments to control cell fate: focus on macromolecular crowding. *Am J Physiol Cell Physiol* **320**: C842-C849.

Zhang RM, Kumra H, Reinhardt DP (2020) Quantification of extracellular matrix fiber systems related to ADAMTS proteins. *Methods Mol Biol* **2043**: 237-250.

Zilberberg L, Todorovic V, Dabovic B, Horiguchi M, Courousse T, Sakai LY, Rifkin DB (2012) Specificity of latent TGF-beta binding protein (LTBP) incorporation into matrix: role of fibrillins and fibronectin. *J Cell Physiol* **227**: 3828-3836.

Zimmermann LA, Correns A, Furlan AG, Spanou CES, Sengle G (2021) Controlling BMP growth factor bioavailability: The extracellular matrix as multi skilled platform. *Cell Signal* **85**: 110071. DOI: 10.1016/j.cellsig.2021.110071.

Discussion with Reviewer

Stuart Cain: Do you think that the use of Ficoll 400 would increase fibrillin-1 deposition in 3D culture situations?

Authors: There is some interesting literature suggesting that MMC mimics 3D culture conditions when generating adipocytes from mesenchymal stem cells. For example, under MMC conditions, Lee *et al.* (2016) observed layered cells with ECM deposition in between, which resembled adipocytes generated in a 3D matrix. In addition, Ranamukhaarachchi *et al.* (2019, additional reference) described the effects of MMC on collagen fibril architecture formed by breast cancer cells embedded in 3D collagen gels, suggesting that MMC exerts its effects in 3D culture as well, given that the molecules can freely diffuse through a 3D matrix. How fibrillin-1 deposition would be changed with MMC under 3D culture conditions is unclear. In fact, most studies of fibrillin-1 deposition use a 2D culture system on tissue culture plastic.

Stuart Cain: Would this approach work in cell types where fibrillin-1 deposition is not so dependant on fibronectin, such as epithelial cells?

Authors: The reviewer raises an interesting question. The work from Baldwin *et al.* (2014, additional reference) showed that epithelial ARPE-19 cells do not require fibronectin for deposition of fibrillin-1, differently from mesenchymal cells (Sabatier *et al.*, 2009). In epithelial cells, an augmentation of fibrillin-1 deposition would be expected through MMC, if the

MMC effect observed in lung fibroblasts is not entirely mediated by increased fibronectin deposition. In other words, this may allow an experimental parsing between effects of MMC on fibronectin and fibrillin-1 deposition in the ECM through application of MMC in epithelial cells.

influences how cells deposit fibrillin microfibrils. *J Cell Sci* **127**: 158-171.

Ranamukhaarachchi SK , Modi RN , Han A , Velez DO , Kumar A , Engler AJ, Fraley SI (2019) Macromolecular crowding tunes 3D collagen architecture and cell morphogenesis. *Biomater Sci* **7**: 618-633.

Additional References

Baldwin AK, Cain SA, Lennon R, Godwin A, Merry CL, Kielty CM (2014) Epithelial-mesenchymal status

Editor's note: The Guest Editor responsible for this paper was Dimitrios Zeugolis.